Supplementary Information

Development of PROTACs for targeted degradation of oncogenic TRK fusions

Saurav Kumar,[‡,a] Jiewei Jiang,[‡,b] Mia S. Donald-Paladino,[a] Joy Chen,[a] Andrea Gutierrez,[c] Alexander J. Federation,[c] Frank Szulzewsky,[d,e] Eric C. Holland,[a] Fleur M. Ferguson,[*,b,f] and Behnam Nabet[*,a,g]

[a] Human Biology Division, Fred Hutchinson Cancer Center, Seattle, WA, 98109, USA

[b] Department of Chemistry and Biochemistry, University of California San Diego, La Jolla, CA, 92093, USA

[c] Talus Bioscience, Inc, Seattle, WA, 98122, USA

[d] Huntsman Cancer Institute, University of Utah, Salt Lake City, UT, 84112, USA

[e] Department of Neurosurgery, Clinical Neurosciences Center, University of Utah, Salt Lake City, UT, 84112, USA

[f] Skaggs School of Pharmacy and Pharmaceutical Sciences, University of California San Diego, La Jolla, CA, 92093, USA

[g] Department of Pharmacology, University of Washington, Seattle, WA, 98195, USA

[‡] Equal contribution

***Correspondence should be addressed to:**

Behnam Nabet, Human Biology Division, Fred Hutchinson Cancer Center, 1100 Fairview Avenue N., Seattle, WA, 98109, USA. Email: bnabet@fredhutch.org

Fleur M. Ferguson, Department of Chemistry and Biochemistry, University of California San Diego, La Jolla, CA, 92093, USA. Email: fmferguson@ucsd.edu

Supplementary Datasets

Dataset S1 | Normalized and scaled quantitative proteomics dataset.

Supplementary Tables

Compound	2D-adherent monolayer IC_{50} (nM)[a]	3D-spheroid suspension IC_{50} (nM)[a]
Entrectinib	0.7	2.0
JWJ-01-375	22.7	31.6
JWJ-01-377	10.8	26.4
JWJ-01-378	6.2	4.2
JWJ-01-392	86.7	109.7
GNF-8625	2.5	5.9
CG-428	0.9	1.0
[a]IC_{50} values are associated with data in Figure 5.		

Table S1 | Antiproliferative effects of TRK inhibitors and PROTACs in KM12 cells cultured as 2D-adherent monolayers or 3D-spheroid suspensions.

Supplementary Figures

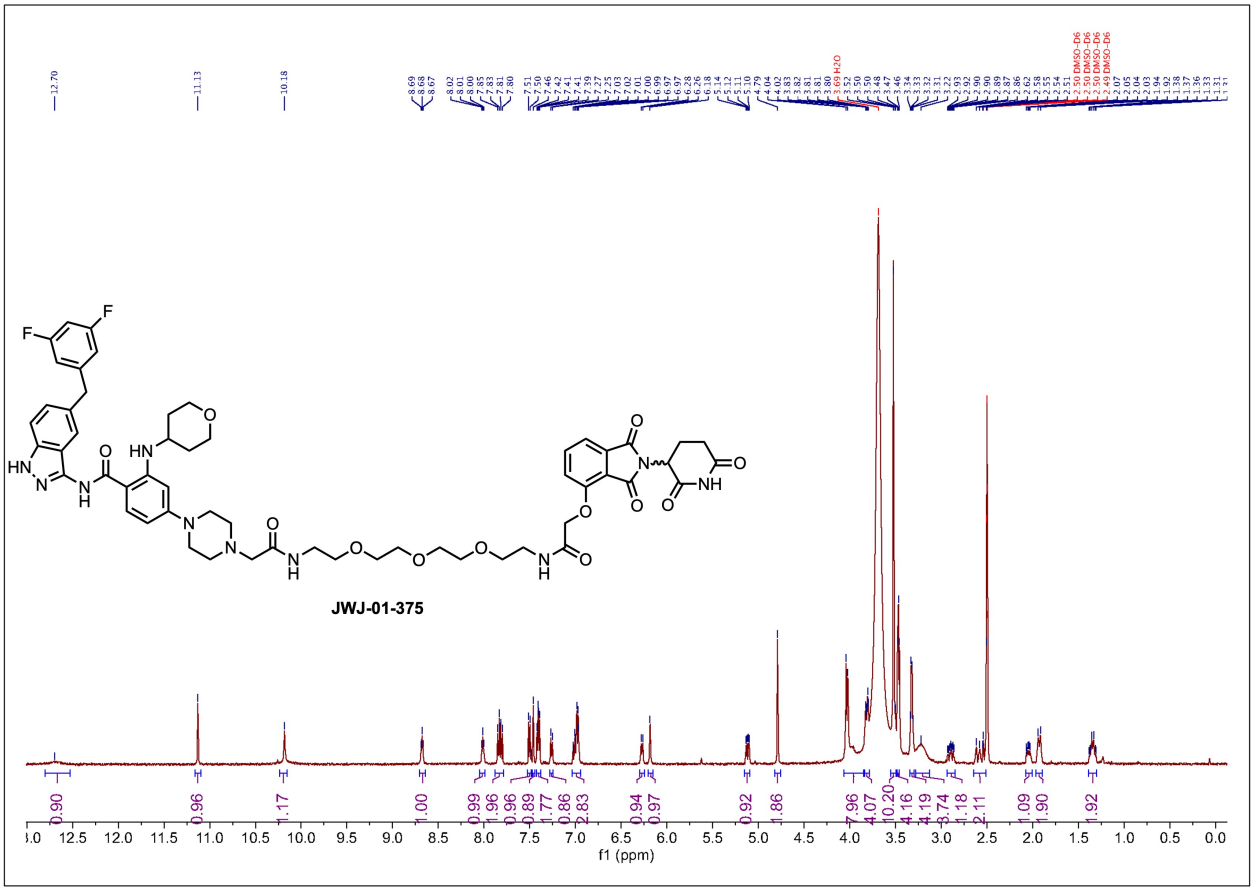

Figure S1 | ^{1}H NMR (500 MHz, DMSO-*d6*) spectrum of JWJ-01-375.

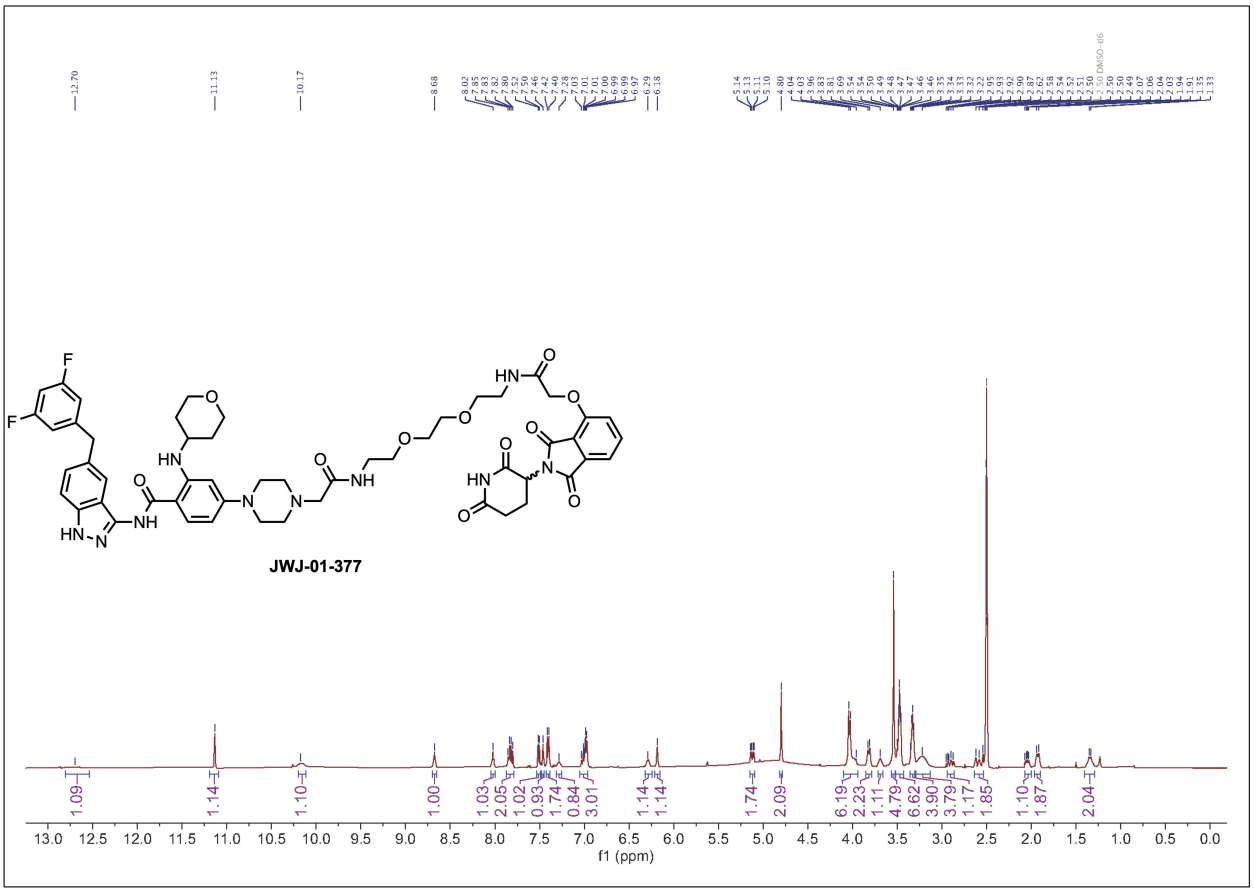

Figure S2 | ^{1}H NMR (500 MHz, DMSO-*d6*) spectrum of JWJ-01-377.

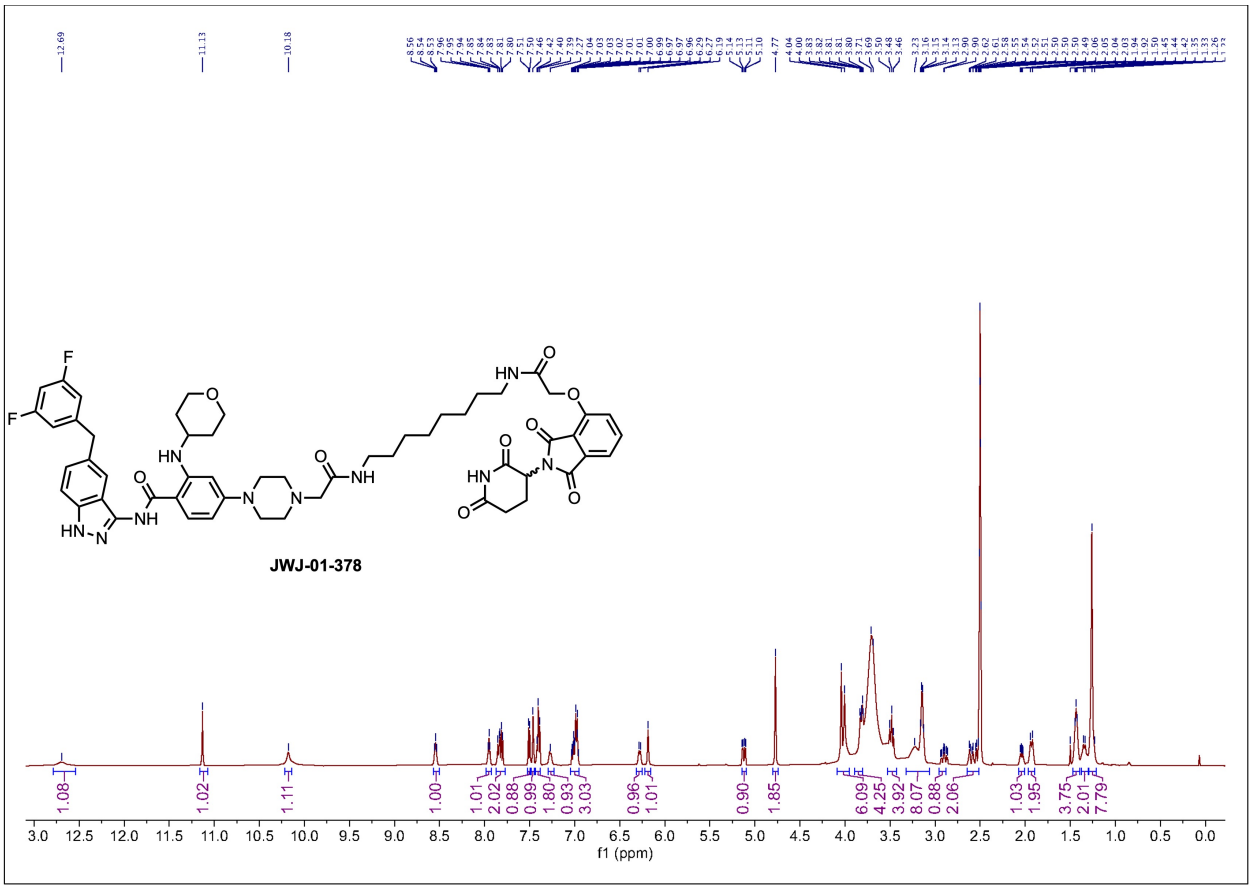

Figure S3 | ^{1}H NMR (500 MHz, DMSO-*d6*) spectrum of JWJ-01-378.

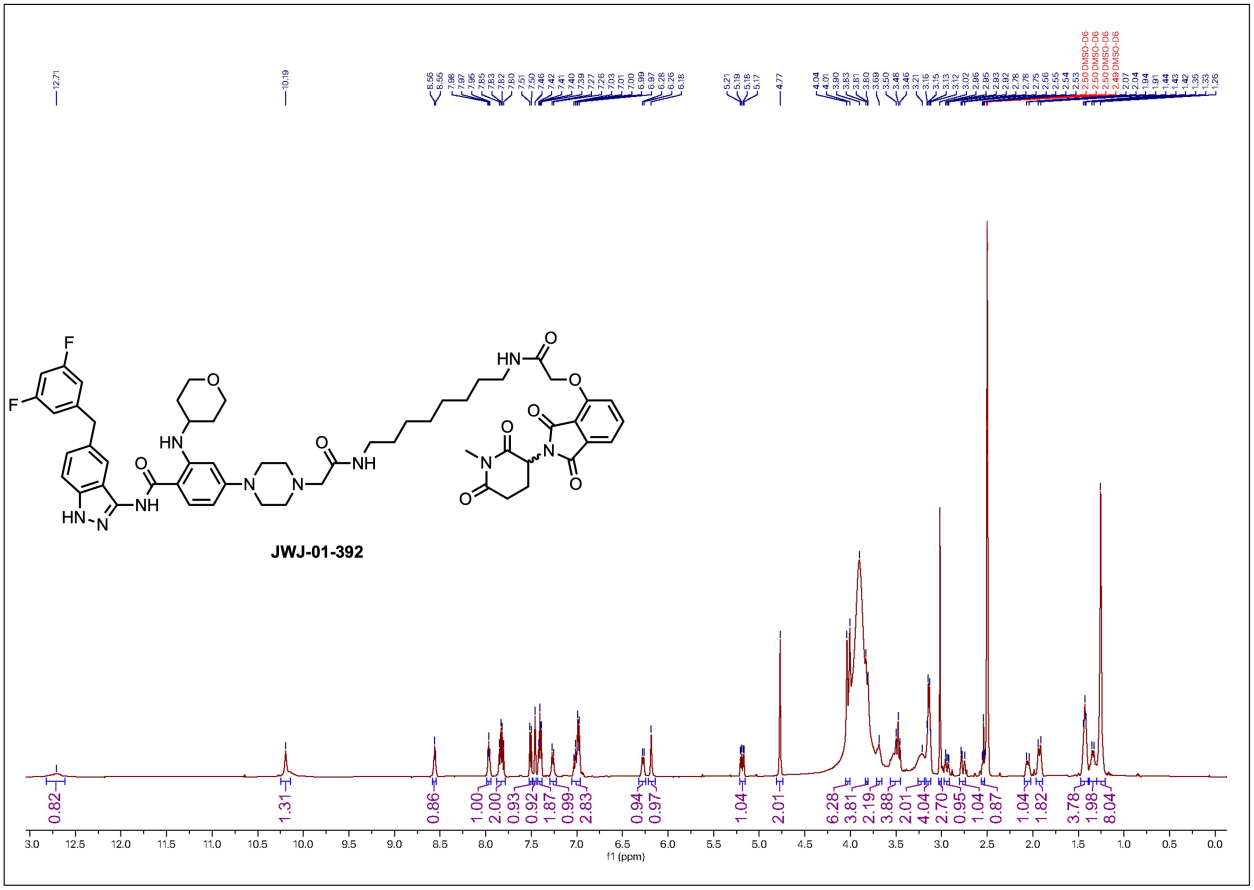

Figure S4 | ^{1}H NMR (500 MHz, DMSO-*d6*) spectrum of JWJ-01-392.

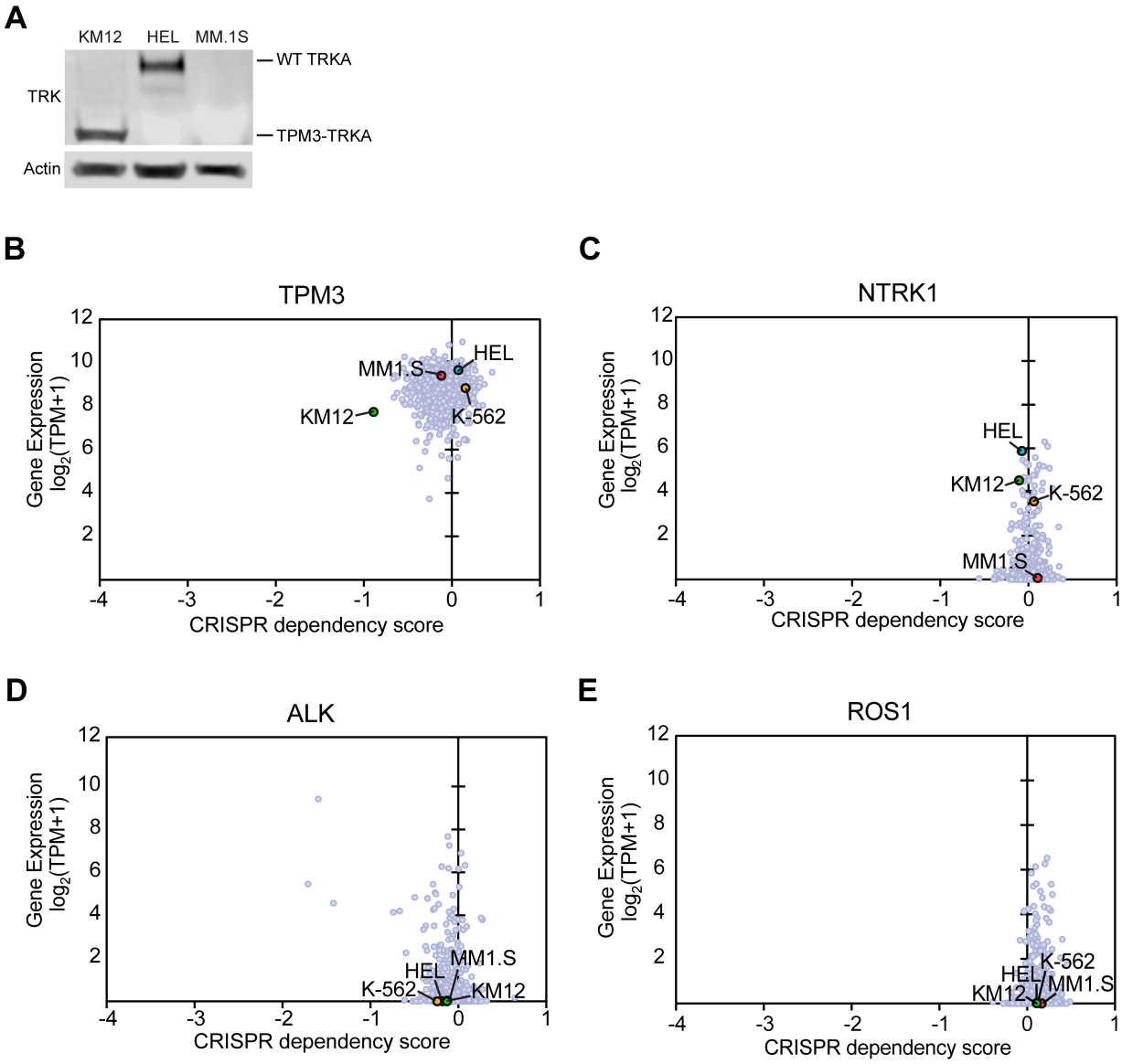

Figure S5 | Expression levels and genetic dependency of the indicated targets. (A) Immunoblot analysis of the indicated cell lines. Data are representative of *n* = 2 independent experiments. (B-E) Scatterplot of *TPM3* (B), *NTRK1* (C), *ALK* (D), and *ROS1* (E) expression levels versus CRISPR screen dependency derived from the depmap.org/portal.

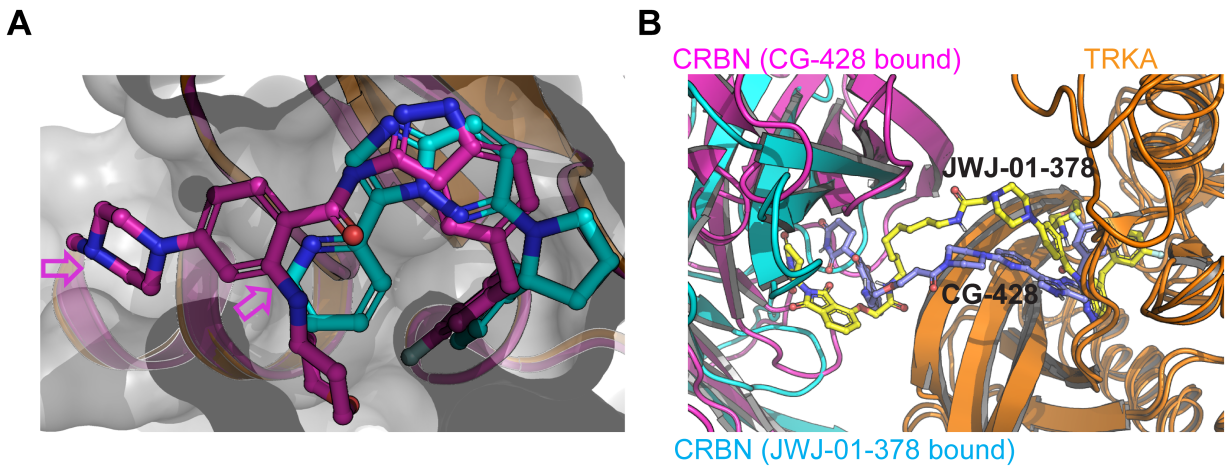

Figure S6 | Docking modeling of inhibitors and PROTACs. (A) The top view of the overlaid co-crystal structures between entrectinib or GNF-8625 and the TRKA kinase domain to highlight that both the *N*-methyl piperazine of entrectinib and the pyridine of GNF-8652 occupy a similar region. (B) The chemical structures of CG-428 and JWJ-01-378 and the superimposition of ternary complexes with TRKA and CRBN. CG-428 and JWJ-01-378 are highlighted in purple and yellow sticks, respectively. CG-428 and JWJ-01-378 bound CRBN proteins are rendered in pink and cyan, respectively.

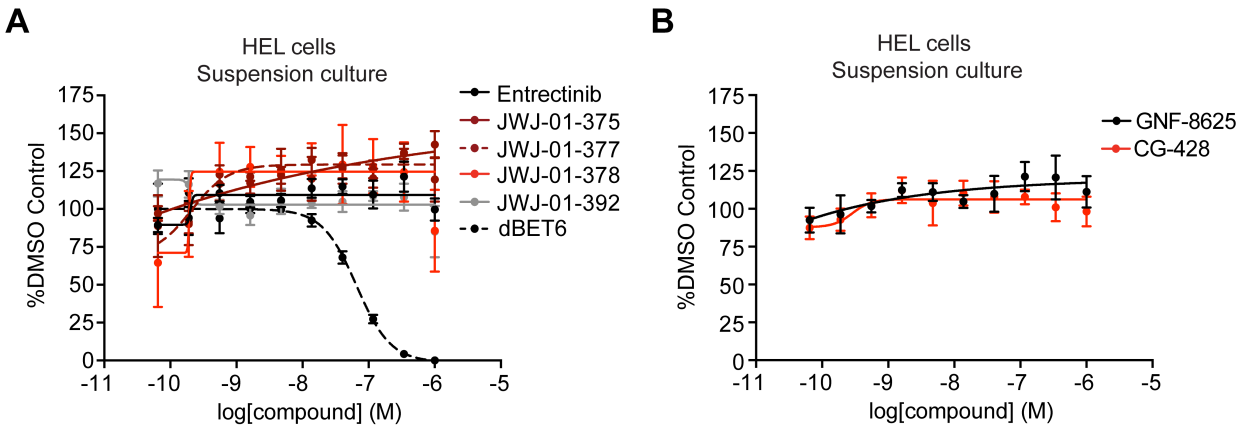

Figure S7 | TRK-targeting compounds do not impact HEL cell viability. (A-B) DMSO-normalized antiproliferation of HEL cells cultured in suspension and treated with indicated compounds for 120 hours. Data are presented as mean ± s.d. of *n* = 4 biologically independent samples and are representative of *n* = 3 independent experiments.

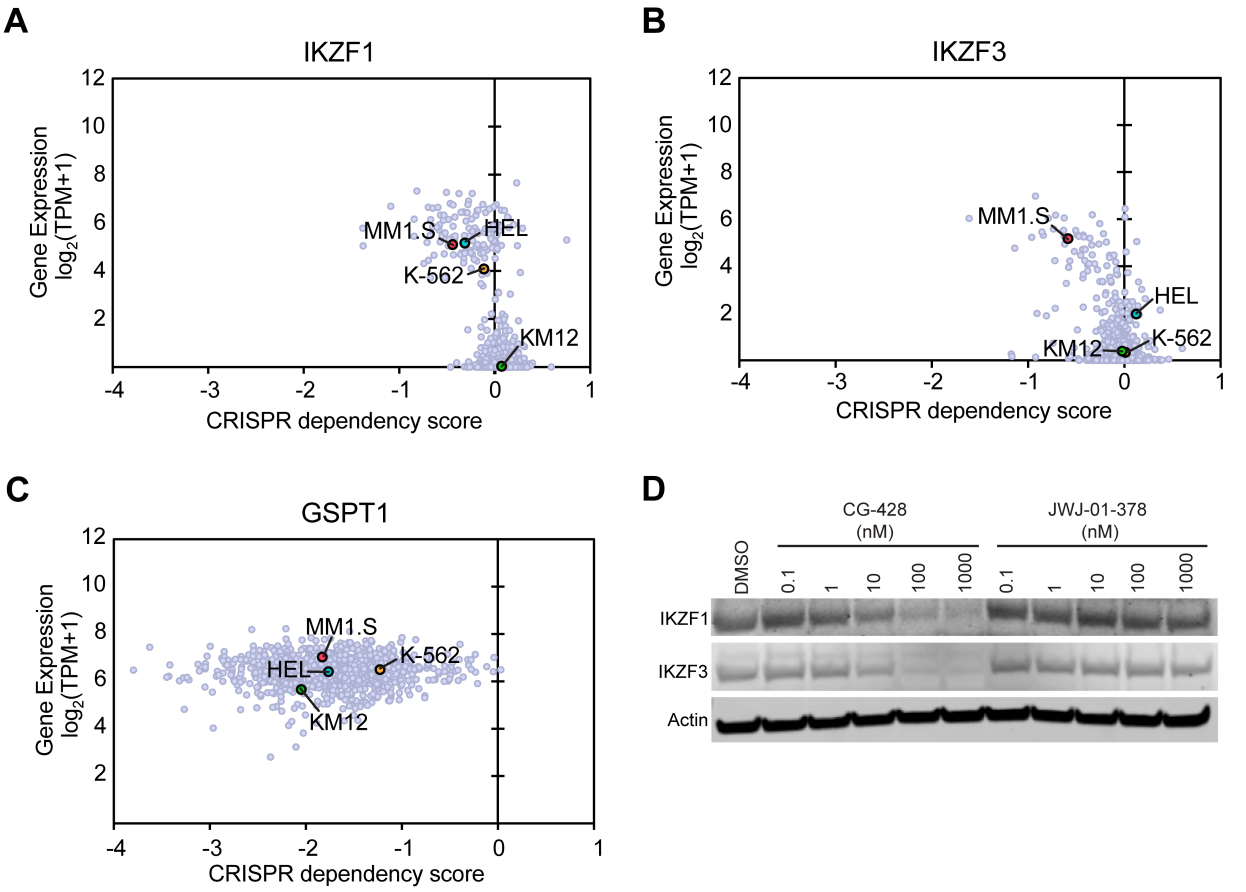

Figure S8 | JWJ-01-378 does not degrade IKZF1 and IKZF3 while CG-428 degrades IKZF1 and IKZF3. (A-C) Scatterplot of *IKZF1* (A), *IKZF3* (B), and *GSPT1* (C) expression levels versus CRISPR screen dependency derived from the depmap.org/portal. (D) Immunoblot analysis of K-562 cells treated with DMSO, CG-428, and JWJ-01-378 at the indicated doses for 24 hours. Data are representative of *n* = 2 experiments.

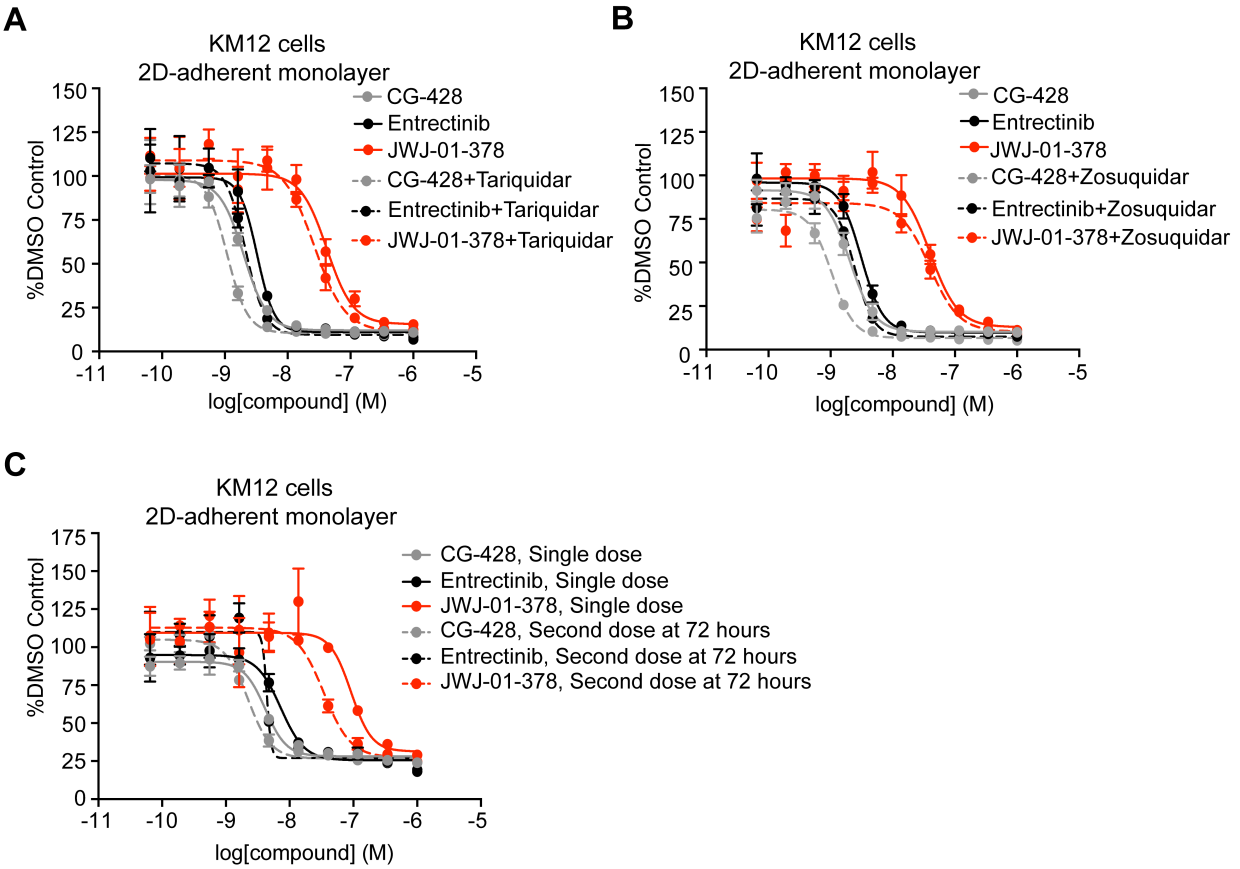

Figure S9 | Drug efflux inhibitors or an additional administration of compound does not improve the biological responses to TRK-targeting inhibitors or PROTACs. (A) DMSO-normalized antiproliferation of KM12 cells cultured as 2D-adherent monolayers and treated with indicated compounds for 120 hours. (B) DMSO-normalized antiproliferation of KM12 cells cultured as 2D-adherent monolayers and treated with indicated compounds for 120 hours. (C) DMSO-normalized antiproliferation of KM12 cells cultured as 2D-adherent monolayers and treated with indicated compounds for a single dose for 120 hours or a second dose at 72 hours before evaluation at 120 hours. Data in (A-C) are presented as mean ± s.d. of *n* = 4 biologically independent samples and are representative of *n* = 3 independent experiments.

Fig. 2A

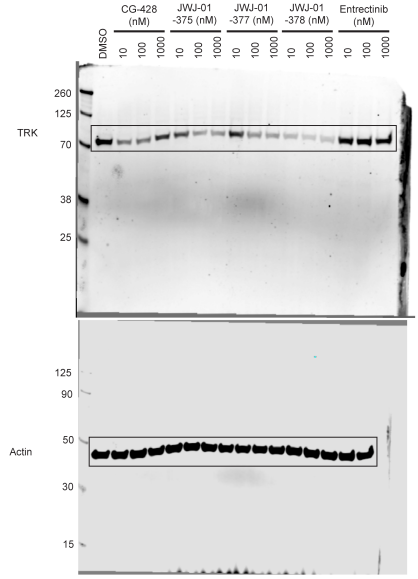

Fig. 2B

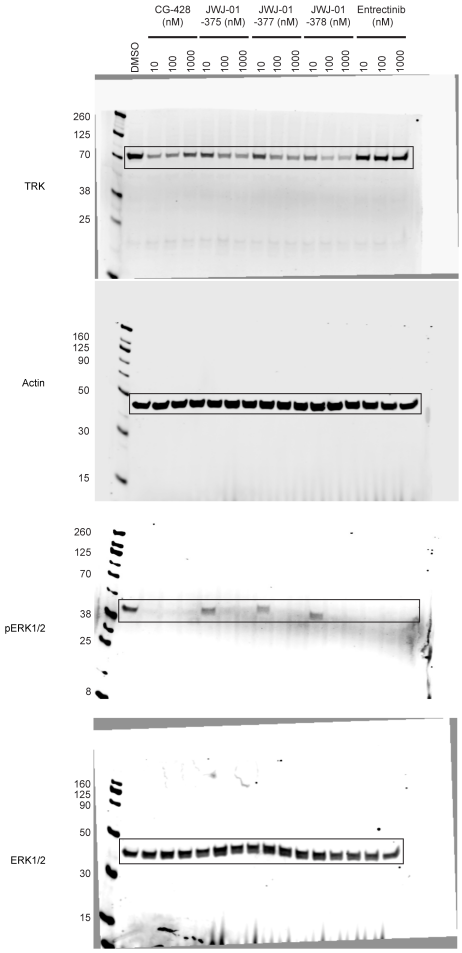

Figure S10 | Uncropped immunoblots for the indicated figures.

Fig. 2C

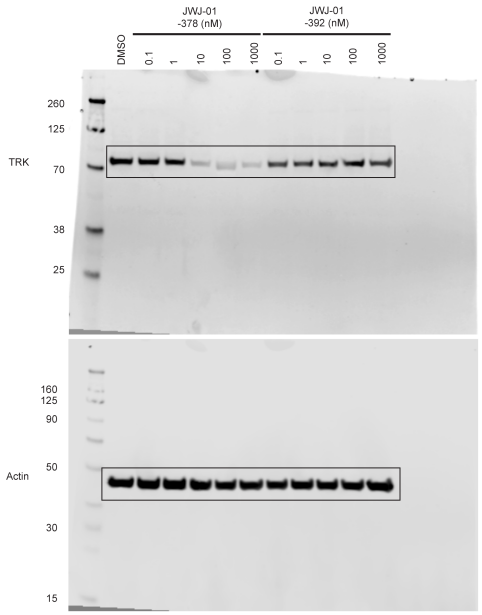

Fig. 2D

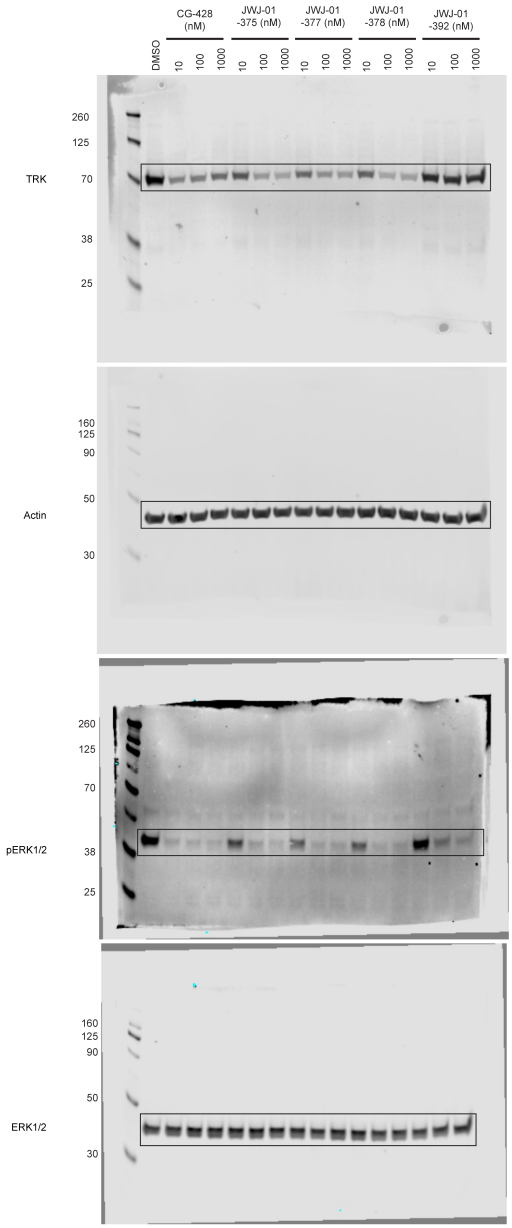

Figure S11 | Uncropped immunoblots for the indicated figures.

Fig. 2E

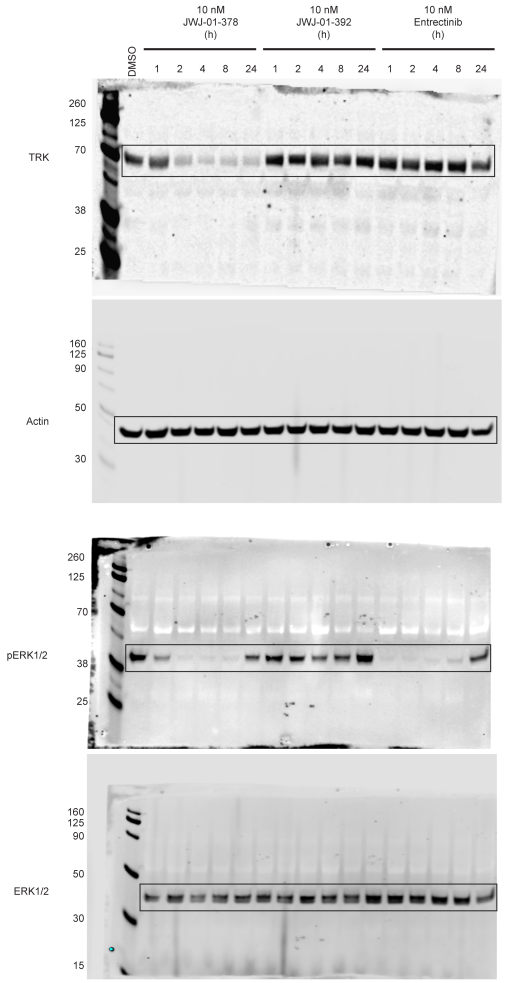

Fig. 2F

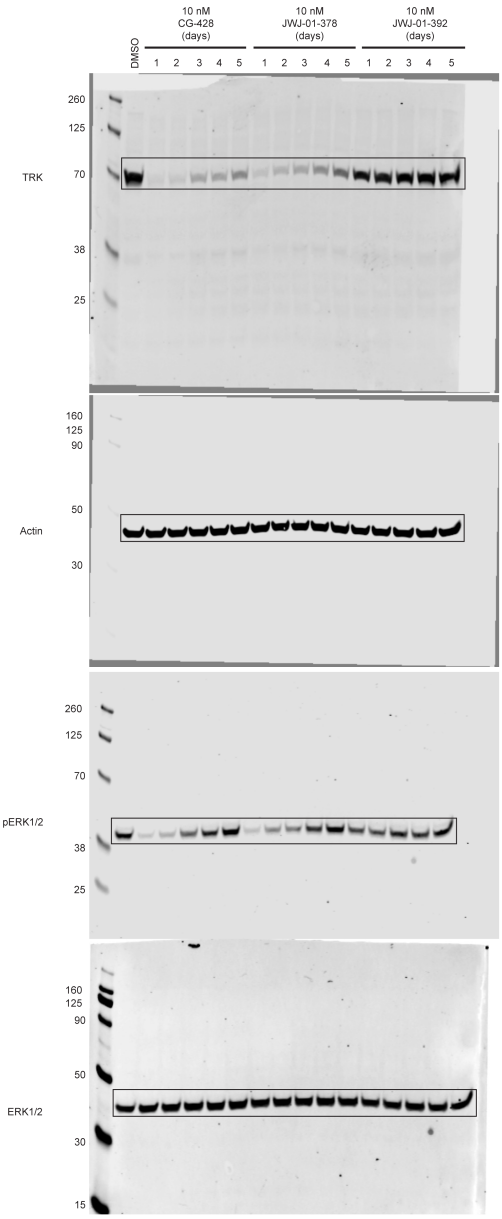

Figure S12 | Uncropped immunoblots for the indicated figures.

Fig. 2G

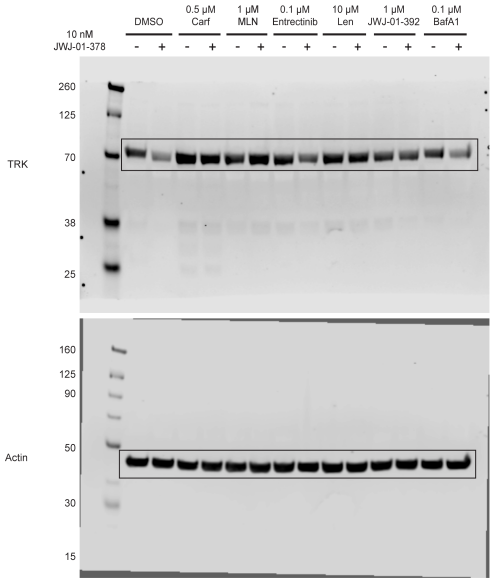

Figure S13 | Uncropped immunoblots for the indicated figures.

Fig. 3A

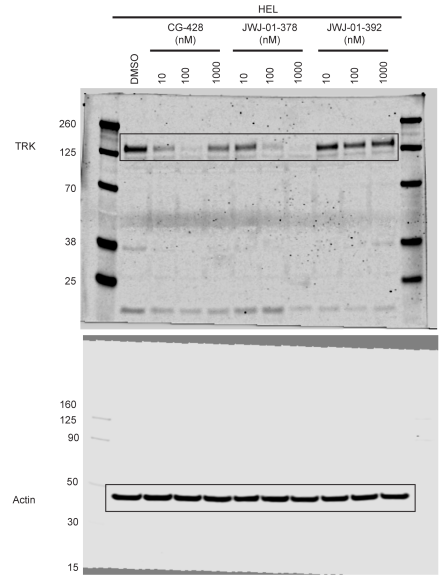

Fig. 3B

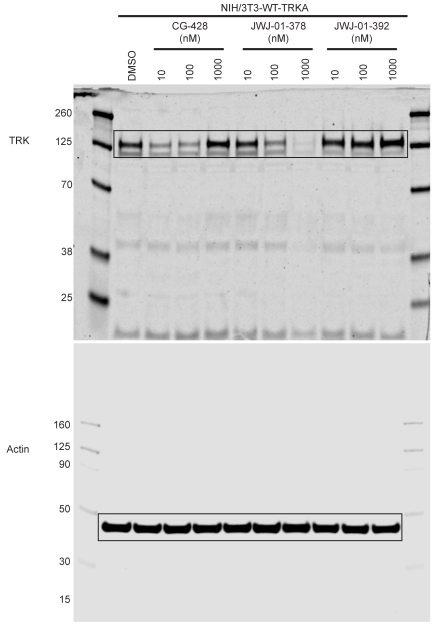

Fig. 3C

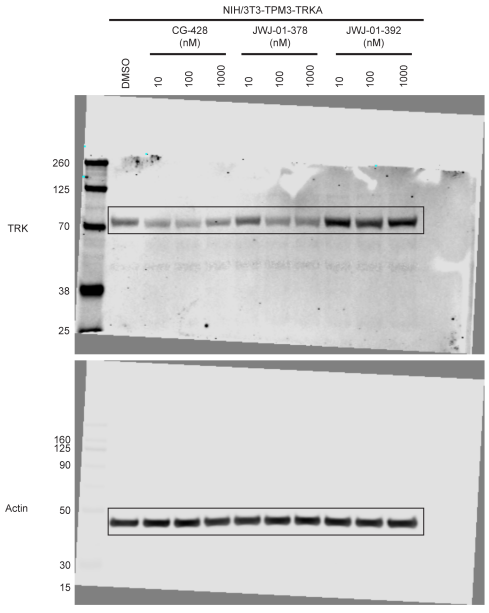

Fig. 3D

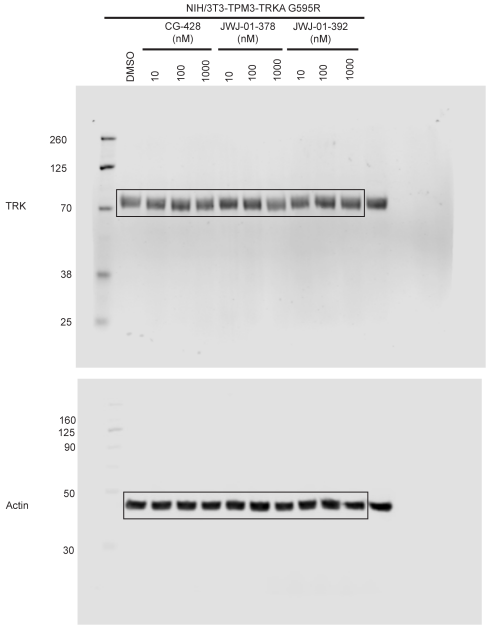

Figure S14 | Uncropped immunoblots for the indicated figures.

Fig. 3E

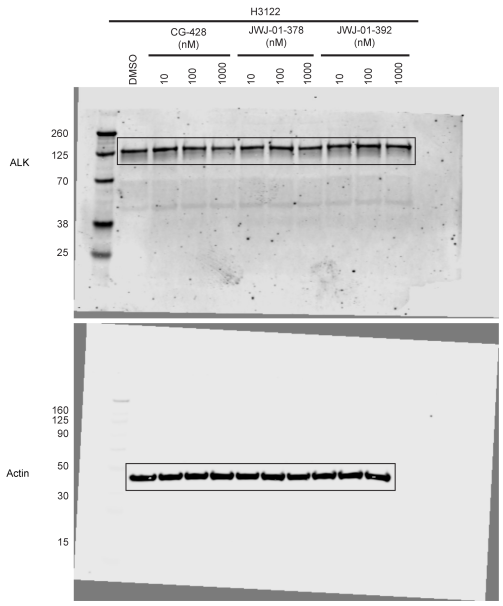

Fig. 3F

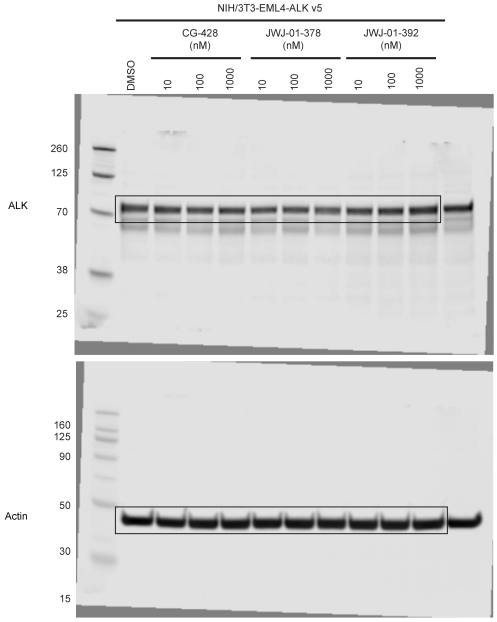

Fig. 3G

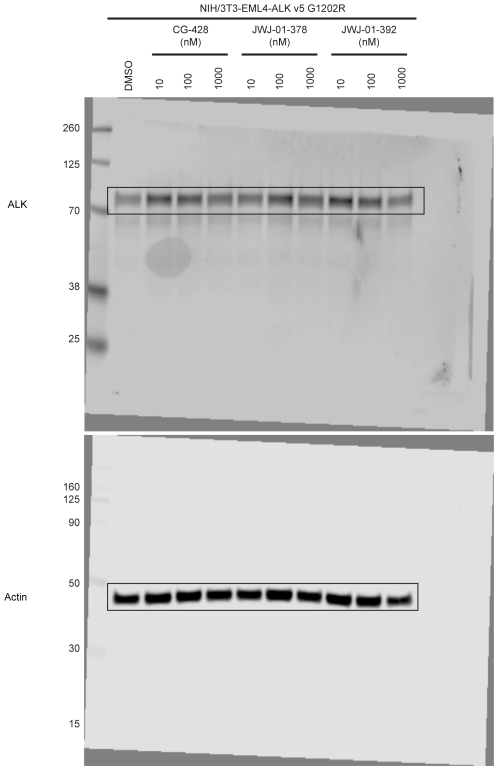

Figure S15 | Uncropped immunoblots for the indicated figures.

Fig. 4A

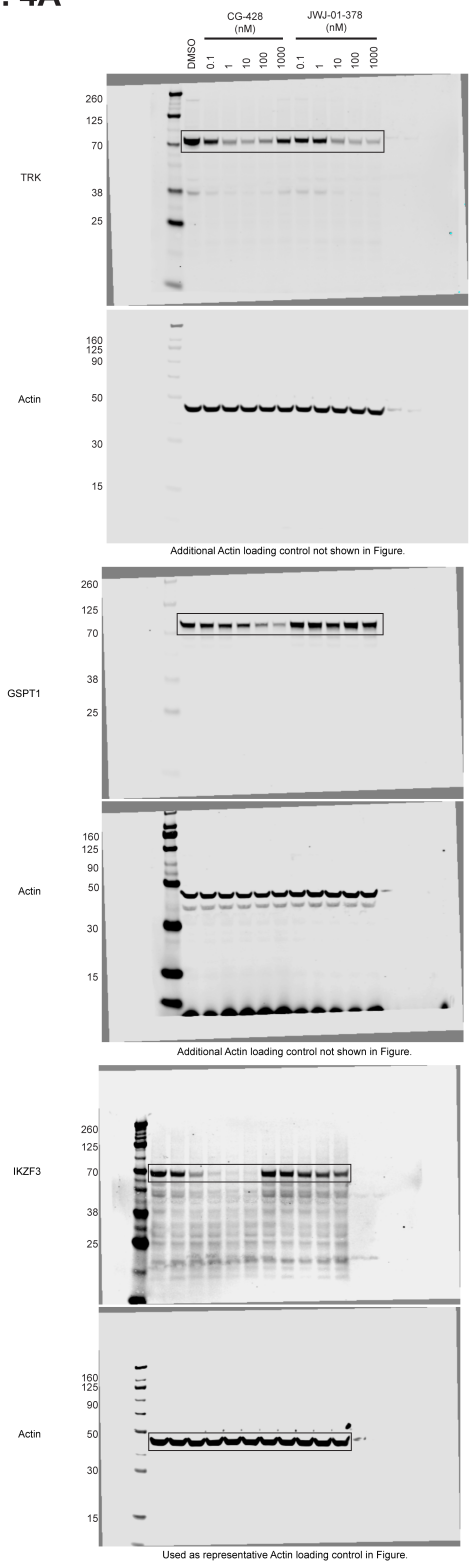

Fig. 4B

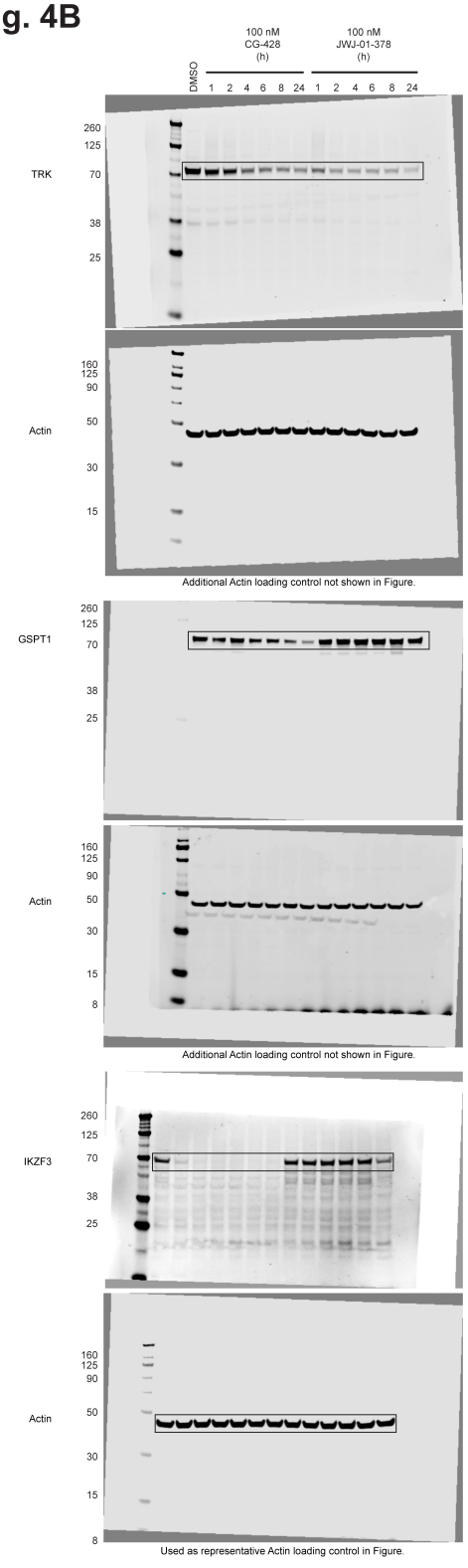

Figure S16 | Uncropped immunoblots for the indicated figures.

Fig. 4C

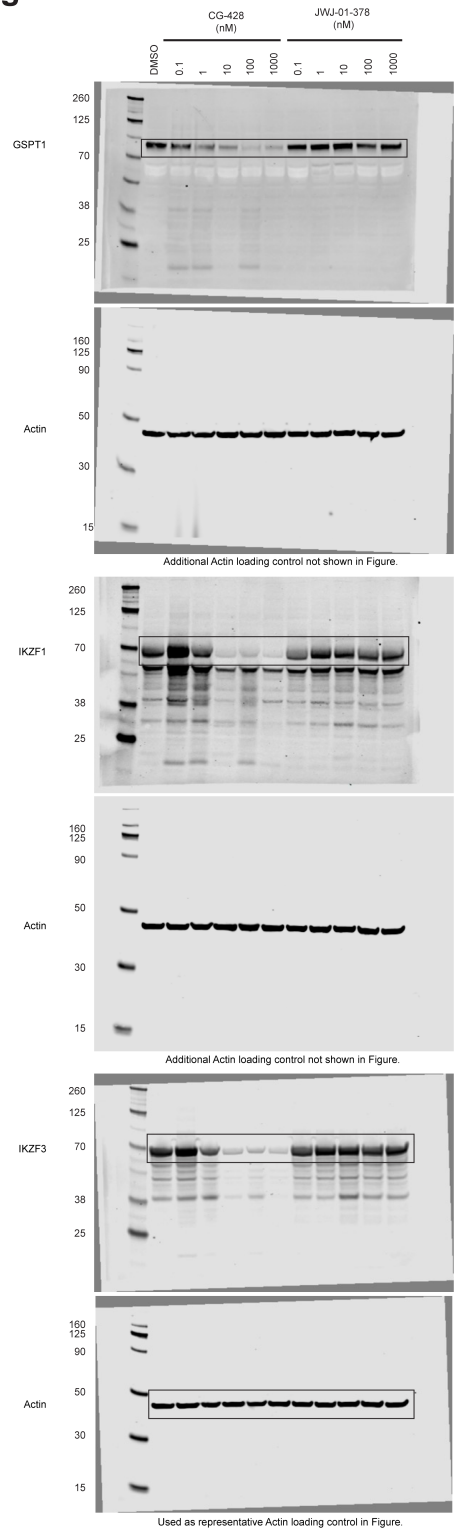

Fig. 4D

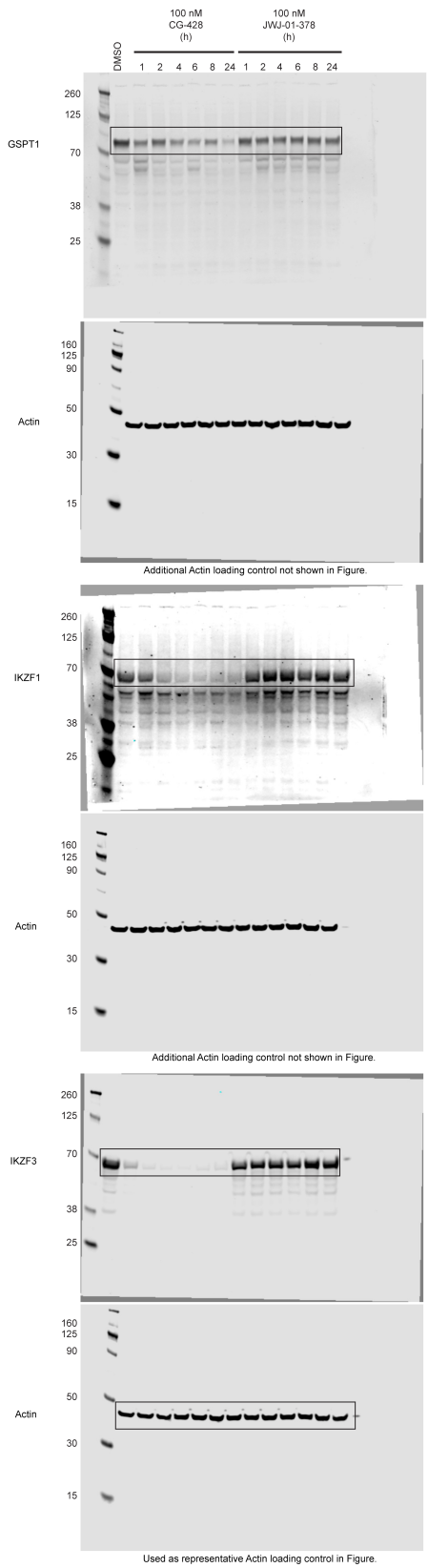

Figure S17 | Uncropped immunoblots for the indicated figures.

Fig. S5A

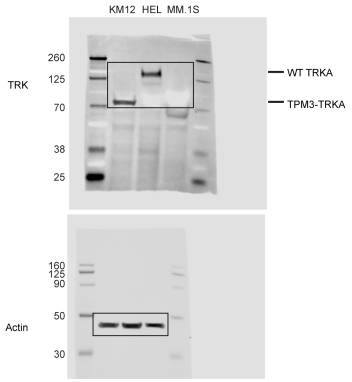

Fig. S8D

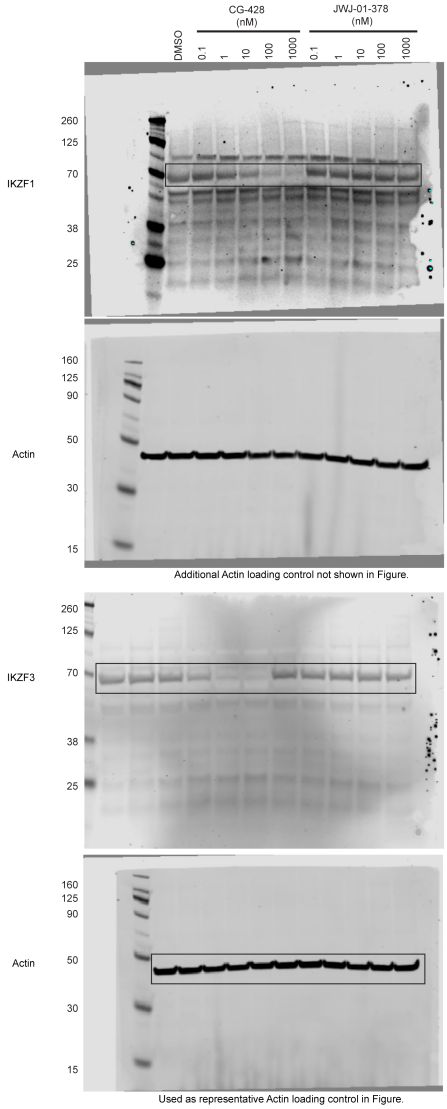

Figure S18 | Uncropped immunoblots for the indicated figures.